JACS
JOURNAL OF THE AMERICAN CHEMICAL SOCIETY
Communication
pubs.acs.org/JACS

Accessibility, Reactivity, and Selectivity of Side Chains within a Channel of *de Novo* Peptide Assembly

Antony J. Burton,[†] Franziska Thomas,[†] Christopher Agnew,[‡] Kieran L. Hudson,[†] Stephen E. Halford,[‡] R. Leo Brady,[‡] and Derek N. Woolfson*[,†,‡]

[†]School of Chemistry, University of Bristol, Bristol BS8 1TS, United Kingdom
[‡]School of Biochemistry, University of Bristol, Bristol BS8 1TD, United Kingdom

Supporting Information

ABSTRACT: *Ab initio* design of enzymes requires precise and predictable positioning of reactive functional groups within accessible and controlled environments of *de novo* protein scaffolds. Here we show that multiple thiol moieties can be placed within a central channel, with approximate dimensions 6 × 42 Å, of a *de novo*, six-helix peptide assembly (CC-Hex). Layers of six cysteine residues are introduced at two different sites ∼6 (the "L24C" mutant) and ∼17 Å (L17C) from the *C*-terminal opening of the channel. X-ray crystal structures confirm the mutant structures as hexamers with internal free thiol, rather than disulfide-linked cysteine residues. Both mutants are hexa-alkylated upon addition of iodoacetamide, demonstrating accessibility and full reactivity of the thiol groups. Comparison of the alkylation and unfolding rates of the hexamers indicates that access is directly through the channel and not via dissociation and unfolding of the assembly. Moreover, neither mutant reacts with iodoacetic acid, demonstrating selectivity of the largely hydrophobic channel. These studies show that it is possible to engineer reactive side chains with both precision and control into a *de novo* scaffold to produce protein-like structures with chemoselective reactivity.

Predictive engineering of novel enzymes has been a goal of protein engineering for some time.[1] An emerging and particularly challenging aspect of such work is the rational, or *ab initio* design of enzyme-like activities into protein scaffolds that are otherwise not known as enzyme frameworks.[2] These scaffolds can be taken from other natural proteins or constructed through *de novo* design.[3] Because it is difficult to envisage matching the complexity, selectivity, efficiency, and dynamics of natural enzymes, such design work is largely an academic exercise at present: it aims to further our fundamental understanding of how enzymes are built and work, and also to test our abilities to engineer biological systems systematically and predictably. That said, an ability to generate protein-based catalysts in this way would have an impact on protein engineering, biotechnology, and synthetic biology, where improved enzymes are being sought, and catalysts for reactions outside the biological arena would be useful.[4]

The current state of the art in *ab initio* enzyme design is to use computational methods to port catalytic constellations of residues into natural protein scaffolds, to test for activity and selectivity, and then to use rounds of mutations (sometimes via directed evolution) to improve these properties.[2b,5] While the exquisite functionalities of natural enzymes are not yet fully matched, good progress is being made using this approach.[2e,6] Much less has been achieved in this area using truly *de novo* protein scaffolds.[7] This is perhaps not surprising as using *de novo* scaffolds brings additional challenges, not least the production of prescribed and stably folded structures in the first place. Nonetheless, the prospect of generating enzyme-like structures and activities *de novo*, and of understanding the role of every amino acid in a designed polypeptide chain, is tantalizing.[8]

With these and other ambitions in mind, we embarked on a synthetic biology approach to the rational design of functional proteins.[9] Our aim is to develop a basis set, or toolkit, of *de novo* protein structures,[10] and then use them as modules to construct more-complex assemblies[11] and display functional residues. To start, we have focused on α-helical bundles, and specifically coiled coils.[12] Thus far, we have delivered a set comprising homo-, di-, tri-, and tetramers, a series of heterodimers with a range of dissociation constants, and a heterotrimer.[10,13] All of these have "stripped-down" sequences; i.e., only the residues important for structural specification and stabilization are defined, leaving the remainder as agnostic side chains (e.g., alanine (Ala, A) or glutamine (Gln, Q)) and free for substitution later in the design process. The basis-set peptides are fully characterized in solution, and in most cases we have determined high-resolution X-ray crystal structures.[10]

One of these structures, a parallel homotetramer (CC-Tet), has been mutated to render the first example of hexameric coiled coil.[14] CC-Hex has a well-defined channel running its entire length, which is open to solvent at both the *N*- and *C*-termini, and is lined exclusively by hydrophobic side chains, isoleucine (Ile, I) and leucine (Leu, L), Figure 1A,B and Table 1. One of these sites, L24, is mutable, accepting side chains including aspartic acid and histidine. Though destabilized, these mutants crystallize as homohexamers closely similar to the parent structures and can be combined to form a stable $(AspHis)_3$ heterohexamer.[14]

We posit that CC-Hex, with its channel, resilience to mutation, and defined structure, presents a good starting point for the rational design of protein function, such as enzyme-like activity. However, open and important questions in this endeavor regard the nature of the channel, and particularly its accessibility to

Received: May 27, 2013
Published: August 7, 2013

 © 2013 American Chemical Society dx.doi.org/10.1021/ja4053027 | *J. Am. Chem. Soc.* 2013, 135, 12524−12527

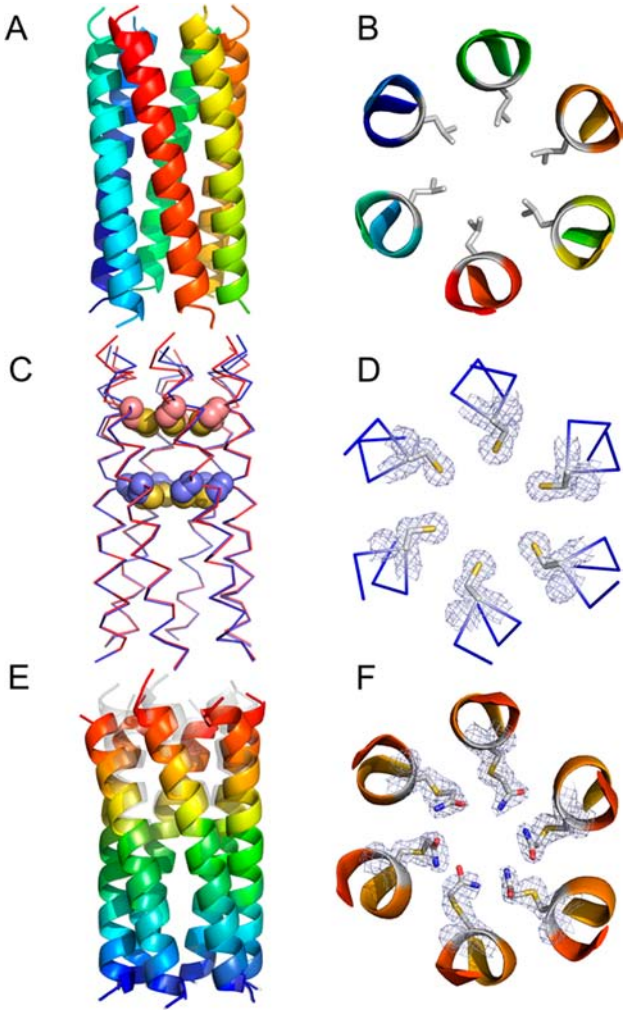

Figure 1. X-ray crystal structures of CC-Hex and the Leu→Cys mutants. (A,B) Orthogonal views of the 2.2 Å structure of CC-Hex (PDB identifier, 3R3K).[14] In B, the side chains of Leu-24 are shown as sticks. (C) Overlay of orthogonal ribbon views of the structures of CC-Hex-L24C (red, 1.6 Å, PDB 4KVT) and CC-Hex-L17C-Y22BrPhe (blue, 1.8 Å, PDB 4KVU), displaying the installed rings of Cys residues. (D) Slice at the 17 position of CC-Hex-L17C displaying the installed corona of Cys side chains. (E) Orthogonal view of the 1.9 Å structure of CC-Hex-L24C-alk-W22BrPhe (PDB 4KVV), overlaid with the backbone of CC-Hex-L24C (gray) to show the slight splaying of the C-termini upon introducing the acetamide functionality. (F) Slice at the 24 position of CC-Hex-L24C-alk-W22BrPhe displaying the installed acetamide side chains. All viewed from the C-terminus (top). In D and F, electron densities ($2F_{obs} - F_{calc}$) for the Cys and Cys-acetamide side chains are shown contoured at 2σ. Images created with PyMOL (http://www.pymol.org/).

substrate and ability to exhaust products. Here we show that it is possible to install reactive cysteine (Cys, C) residues within the channel, where they are accessible to modification by molecules directly entering the channel. Cys was selected because of its nucleophilic side chain, and as it is represented within the active site of many enzymes.[15]

Two potential Leu→Cys mutants were modeled using PyMOL, Figure S1A. These were made at the *a*-sites of the third and fourth heptad repeats of the CC-Hex sequence, Table 1, which placed them about half and three-quarters of the way along the channel, respectively, Figure 1C. Leu→Cys mutations appeared to be accommodated at both positions on all six helices,

Table 1. Sequences of the *de Novo*-Designed CC-Hex Peptides

Name	Peptide sequences and heptad register *gabcdefgabcdefgabcdefgabcdef*
CC-Hex	Ac-GELKAIAQELKAIAKELKAIAWELKAIAQGAG-NH_2
CC-Hex-L17C	Ac-GELKAIAQELKAIAKE**C**KAIAYELKAIAQGAG-NH_2
CC-Hex-L24C	Ac-GELKAIAQELKAIAKELKAIAWE**C**KAIAQGAG-NH_2

and without the likelihood of forming interhelix disulfide bonds. On this basis, two mutants, CC-Hex-L17C and CC-Hex-L24C, were synthesized by solid-phase peptide synthesis, purified by reverse-phase HPLC, and confirmed by MALDI-TOF-MS, Figure S2A,B. As judged by circular dichroism (CD) spectroscopy, both peptides were α-helical in solution and displayed sigmoidal thermal denaturation when monitored at 222 nm, corresponding to T_M = 67 and 78 °C for CC-Hex-L17C and CC-Hex-L24C, respectively, Figure 2. Dynamic light scattering was

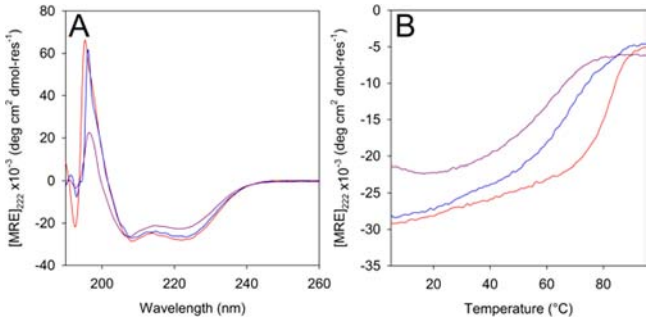

Figure 2. Biophysical characterization of the CC-Hex-L→C variants in solution. (A) CD spectra at 20 °C for CC-Hex-L17C (blue), CC-Hex-L24C (red), and CC-Hex-L24C-alk (purple). α-Helicities were calculated as ~85% for CC-Hex-L17C and CC-Hex-L24C, and ~65% for CC-Hex-L24C-Alk. (B) Thermal denaturation curves for the three variants monitored by the change in CD signal at 222 nm (same color scheme as for panel A). The T_M values derived from these curves were 67 (CC-Hex-L17C), 78 (CC-Hex-L24C), and 56 °C (CC-Hex-L24C-alk). Conditions: 50 μM peptide, phosphate-buffered saline (PBS, pH 7.4), tris(2-carboxyethyl)phosphine (TCEP, 0.5 mM).

used to examine the apparent size of the constructs in solution and indicated small discrete assemblies consistent with hexamers, Figure S3. This oligomeric state was confirmed by sedimentation-equilibrium experiments performed by analytical ultracentrifugation, with experimental curves readily fitting models for single, ideal species with masses corresponding to hexamers for both mutants, Figure S4A,B.

The assemblies were characterized unambiguously as parallel, hexameric coiled-coil architectures by X-ray crystallography, Table S1. The 1.8 and 1.6 Å resolution crystal structures of CC-Hex-L17C-Y22BrPhe and CC-Hex-L24C, respectively, were determined by molecular replacement using the parent CC-Hex structure as a search model, Figure 1C,D. [The Tyr/Trp→BrPhe mutants were made simply to assist with phasing crystallographic diffraction data, should that have been needed.] The characterization and X-ray crystal structure of CC-Hex-L17C provide the first example of a benign mutation of CC-Hex in the central heptad. In both structures, the designed coronas of Cys residues at the heart of the suprastructures were clear, Figure 1D. As with the parent assembly, solvent-like electron density was evident along the central channels in both structures, and this was modeled, by best fit, to water molecules. Importantly, the introduced Cys residues were not oxidized to form disulfide

dx.doi.org/10.1021/ja4053027 | J. Am. Chem. Soc. 2013, 135, 12524−12527

bridges. Furthermore, no oxidation was observed by MALDI-TOF-MS after 7 days in solution and in the absence of small-molecule reducing agents. The minimum S_γ–S_γ distance from the crystal structures was 4.4 Å, compared to the expected disulfide bond length of 2.05 Å, explaining why oxidation was not observed. Thus, the constructs exist as stable hexamers with six potentially reactive Cys residues in their central channels.

After biophysical characterization, the reactivities of the installed Cys side chains were investigated. Among other methods,[16] accessibility of Cys residues in folded proteins has been probed by reaction with small-molecule alkylating agents such as iodoacetamide and iodoacetic acid.[17] Encouragingly, in the Leu→Cys systems both Cys mutants reacted chemoselectively with an excess of iodoacetamide to render the hexa-alkylated thioether product, as judged by HPLC and MS, Figure S5A,B. Kinetic analyses of the pseudo-first-order rate constants (k_{app}) at various excess concentrations of iodoacetamide allowed rates of alkylation (k_{alk}) for both constructs to be determined as $\sim 2 \times 10^{-2}$ M^{-1} s^{-1}, Figure 3A,B. [The rate for CC-Hex-L17C was the larger, a point we return to below.] For comparison, a random-coil control peptide (Ac-GAYECKAIAKELGAG-NH_2) was synthesized and found to react with a half-life of 7 s under similar conditions, equating to a rate of ~ 2 M^{-1} s^{-1}, Figure S6; i.e., ~100× faster than the full-length mutants.

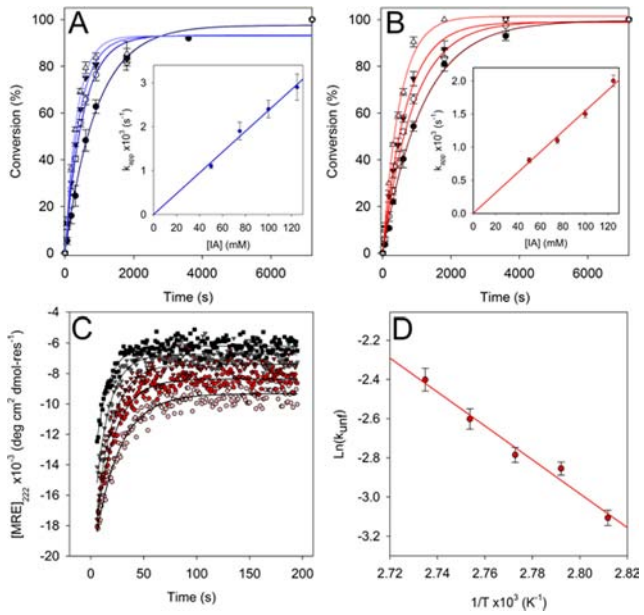

Figure 3. Kinetics of alkylation and unfolding reactions in the CC-Hex variants. (A,B) Reaction profiles for the reaction of CC-Hex-L17C (A) and CC-Hex-L24C (B) with 50 (●), 75 (○), 100 (▼), and 125 mM (Δ) iodoacetamide at 20 °C obtained from HPLC peak-area integration (Figure S5A,B). Inset: Linearization of the pseudo-first-order rate constants (k_{app}) obtained at excess concentrations of iodoacetamide, $k_{alk,L17C} = 2.4 \times 10^{-2} \pm 5 \times 10^{-4}$ M^{-1} s^{-1}, $k_{alk,L24C} = 1.6 \times 10^{-2} \pm 3 \times 10^{-4}$ M^{-1} s^{-1}. (C) Loss of helicity measured by CD spectroscopy of CC-Hex-L24C during T-shock experiments after rapid heating from 20 to 82.5 (pink ○), 85 (red ○), 87.5 (red ▽), 90 (gray ▽), and 92.5 °C (black ■). (D) Arrhenius plot for the unfolding (k_{unf}) rates for CC-Hex-L24C. Extrapolation from the linear line of best fit returned $k_{unf,20\ °C} = 2.6 \times 10^{-4} \pm 2.1 \times 10^{-4}$ s^{-1}, corresponding to a half-life for unfolding of ~45 min; ~60× less than the rate of alkylation measured in B. Conditions: 50 μM peptide, 0.5 mM TCEP, PBS, pH 7.4.

With iodoacetic acid, no detectable reactions occurred with either folded mutant during the length of the experiments (120 h). This provides an initial example of substrate selectivity within a designed protein channel, with the charged and solvated carboxylate functionality presumably unable to enter the hydrophobic channel of the assembly at pH 7.4.

From the difference in rates of alkylation of the folded and unfolded peptides, it is tempting to conclude that for the folded mutants the slower reactions are regulated via accessibility of the iodoacetamide into the channel. However, a second potential reaction pathway can be envisaged in which the assemblies first unfold, followed by rapid reaction with the electrophile. To test which mechanism operates, the unfolding rates of the constructs (k_{unf}) were determined using temperature-shock (T-shock) experiments followed by CD spectroscopy (Figures 3C,D and S7): starting in the folding state, the temperature of a sample was raised rapidly above the T_M of the variant; the rate of loss of the CD signal was then measured; a series of rates were determined for each mutant at different final temperatures; and Arrhenius plots of these rates against $1/T$ allowed extrapolation to give unfolding rates at 20 °C, for comparison with the rates of alkylation (assuming a linear relationship over this temperature range). From these experiments we calculated $k_{unf,20\ °C} = 7.9 \times 10^{-4}$ for CC-Hex-L17C and 2.6×10^{-4} s^{-1} for CC-Hex-L24C, corresponding to half-lives of 11 and 45 min, respectively, at 20 °C. The rate of alkylation of CC-Hex-L24C was 60× faster than that of unfolding. Thus, the Cys side chains must be accessed by iodoacetamide predominantly with the peptide in its assembled hexameric state, i.e., directly via the channel.

One caveat of this model is that the structures, stabilities, and rates of unfolding of the CC-Hex-L→C mutants are likely to change upon alkylation; indeed, potentially there is a spectrum of properties for each mutant depending on the degree of alkylation. To test the extreme of these possibilities, the fully alkylated form of CC-Hex-L24C (CC-Hex-L24C-alk) was isolated and characterized: CD spectra at 20 °C showed that CC-Hex-L24C-alk maintained α-helical secondary structure, albeit with a 20% loss in helicity, Figure 2A; thermal denaturation curves were sigmoidal, T_M = 56 °C, Figure 2B; and sedimentation-equilibrium data fitted a single, ideal, hexameric species, Figure S4C. Together, these data indicate a stably folded hexamer in solution. Furthermore, that the steric bulk of six acetamide groups can be tolerated within the lumen of CC-Hex was confirmed by determining a 1.9 Å crystal structure of CC-Hex-L24C-alk-W22BrPhe, Figure 1E,F. This showed some fraying of the *C*-termini of the helices, accounting for the loss in helicity by CD spectroscopy, Figure 2A. It also revealed ordered acetamide groups covalently bound to all six Cys side chains, Figure 1F. Finally, as another extreme test of the alternative alkylation mechanism, for CC-Hex-L24C-alk we determined $k_{unf,20\ °C} = 1.4 \times 10^{-3}$ s^{-1} ($t_{1/2,unf} \approx 8$ min), which remains slower than the rate of alkylation, Figure S8.

By examining both extremes, for CC-Hex-L24C at least, it is evident that alkylation of the installed Cys residues within the channel of CC-Hex occurs predominantly directly through the channel, rather than indirectly via complete unfolding of the assembly. Of course, breathing mechanisms cannot be discounted by our studies, but would seem unlikely too as they would require gross changes to the protein structure to reveal the internal Cys residues.

In comparison, hexa-alkylated CC-Hex-L17C (CC-Hex-L17C-alk) was largely unfolded by CD scans at 50 μM peptide, and showed only partial α-helical folding at 270 μM (Figure S9). The molecular mass in solution was equivalent to ~6 times the monomer mass, but residuals from single-ideal-species or

dx.doi.org/10.1021/ja4053027 | J. Am. Chem. Soc. 2013, 135, 12524–12527

equilibrium models were poor, Figure S4D. Thus, CC-Hex does not fully tolerate bulky substituents halfway along its channel, at least not at what would be considered *useful* peptide concentrations ($\leq\mu$M). This is not to say that changes and reactions cannot be made more centrally; clearly they can, but not fully at all six sites. Returning to the alkylation rate: this is slightly higher for CC-Hex-L17C than CC-Hex-L24C (Figure 3A,B), consistent with a change in mechanism of alkylation as the reaction proceeds and the complex becomes more destabilized; i.e., the more-alkylated variants may well be accessing the unfolding state to give a higher rate of alkylation.

In summary, we report the first example of reactivity and selectivity within the lumen of a *de novo* peptide assembly with an accessible central channel: alkylation of precisely installed cysteine residues proceeds to completion with the construct maintaining its quaternary structure. These reactions, which proceed in water at 20 °C and pH 7.4, are slowed compared with that for a random-coil, Cys-containing, control peptide, but faster than would be expected for a two-step mechanism involving (i) channel disassembly and (ii) alkylation of the exposed thiol groups. Thus, we conclude that access of the reactant is predominantly directly through the assembled channel. Moreover, the channel discriminates for a nonpolar reactant (iodoacetamide) over one with a formal charge (iodoacetic acid). Clearly, we have not made anything enzyme-like in this study; we have simply modified internally located thiol moieties in a *de novo* protein framework. Nonetheless, in so doing we have begun to demonstrate some of the key elements that will be required to construct enzyme-like functions *de novo*: (1) precise and predictable placement of functional groups within a *de novo* protein framework; (2) controlled reactivity of these groups (in this case, incorporating thiol groups that act as nucleophiles, but do not form local disulfide bonds); and (3) discrimination of different reactants ("substrates"). This investigation represents the first step toward functional variants of CC-Hex. Specifically, it potentially adds *de novo* polypeptide scaffolds to the natural structures that are currently employed as the basis for *ab initio* enzyme design.

■ ASSOCIATED CONTENT

Supporting Information

Experimental details and characterization data. This material is available free of charge via the Internet at http://pubs.acs.org.

■ AUTHOR INFORMATION

Corresponding Author

d.n.woolfson@bristol.ac.uk

Notes

The authors declare no competing financial interest.

■ ACKNOWLEDGMENTS

A.J.B. and K.L.H. are supported by the EPSRC-funded Bristol Chemical Synthesis Centre for Doctoral Training. F.T. is funded by the Leverhulme Trust (RPG-2012-536). We thank Drs. Nick Burton and Drew Thomson for helpful discussions. X-ray diffraction data collection was carried out at the Diamond Light Source.

■ REFERENCES

(1) (a) Knowles, J. R. *Nature* **1991**, *350*, 121. (b) Thorn, S. N.; Daniels, R. G.; Auditor, M.-T. M.; Hilvert, D. *Nature* **1995**, *373*, 228.

(2) (a) Jiang, L.; Althoff, E. A.; Clemente, F. R.; Doyle, L.; Röthlisberger, D.; Zanghellini, A.; Gallaher, J. L.; Betker, J. L.; Tanaka, F.; Barbas, C. F.; Hilvert, D.; Houk, K. N.; Stoddard, B. L.; Baker, D. *Science* **2008**, *319*, 1387. (b) Privett, H. K.; Kiss, G.; Lee, T. M.; Blomberg, R.; Chica, R. A.; Thomas, L. M.; Hilvert, D.; Houk, K. N.; Mayo, S. L. *Proc. Natl. Acad. Sci. U.S.A.* **2012**, *109*, 3790. (c) Richter, F.; Blomberg, R.; Khare, S. D.; Kiss, G.; Kuzin, A. P.; Smith, A. J. T.; Gallaher, J.; Pianowski, Z.; Helgeson, R. C.; Grjasnow, A.; Xiao, R.; Seetharaman, J.; Su, M.; Vorobiev, S.; Lew, S.; Forouhar, F.; Kornhaber, G. J.; Hunt, J. F.; Montelione, G. T.; Tong, L.; Houk, K. N.; Hilvert, D.; Baker, D. *J. Am. Chem. Soc.* **2012**, *134*, 16197. (d) Smith, A. J. T.; Müller, R.; Toscano, M. D.; Kast, P.; Hellinga, H. W.; Hilvert, D.; Houk, K. N. *J. Am. Chem. Soc.* **2008**, *130*, 15361. (e) Kiss, G.; Çelebi-Ölçüm, N.; Moretti, R.; Baker, D.; Houk, K. N. *Angew. Chem., Int. Ed.* **2013**, *52*, 5700.

(3) Wörsdörfer, B.; Henning, L. M.; Obexer, R.; Hilvert, D. *ACS Catal.* **2012**, *2*, 982.

(4) (a) Siegel, J. B.; Zanghellini, A.; Lovick, H. M.; Kiss, G.; Lambert, A. R.; St.Clair, J. L.; Gallaher, J. L.; Hilvert, D.; Gelb, M. H.; Stoddard, B. L.; Houk, K. N.; Michael, F. E.; Baker, D. *Science* **2010**, *329*, 309. (b) Bjelic, S.; Nivón, L. G.; Çelebi-Ölçüm, N.; Kiss, G.; Rosewall, C. F.; Lovick, H. M.; Ingalls, E. L.; Gallaher, J. L.; Seetharaman, J.; Lew, S.; Montelione, G. T.; Hunt, J. F.; Michael, F. E.; Houk, K. N.; Baker, D. *ACS Chem. Biol.* **2013**, *8*, 749. (c) Hyster, T. K.; Knörr, L.; Ward, T. R.; Rovis, T. *Science* **2012**, *338*, 500. (d) Coelho, P. S.; Brustad, E. M.; Kannan, A.; Arnold, F. H. *Science* **2013**, *339*, 307.

(5) (a) Richter, F.; Leaver-Fay, A.; Khare, S. D.; Bjelic, S.; Baker, D. *PLoS ONE* **2011**, *6*, e19230. (b) Nanda, V.; Koder, R. L. *Nat. Chem.* **2010**, *2*, 15.

(6) Kries, H.; Blomberg, R.; Hilvert, D. *Curr. Opin. Chem. Biol.* **2013**, *17*, 221.

(7) (a) Johnsson, K.; Allemann, R. K.; Widmer, H.; Benner, S. A. *Nature* **1993**, *365*, 530. (b) Armstrong, C. T.; Watkins, D. W.; Anderson, J. L. R. *Dalton Trans.* **2013**, *42*, 3136. (c) Kaplan, J.; DeGrado, W. F. *Proc. Natl. Acad. Sci. U.S.A.* **2004**, *101*, 11566.

(8) Koder, R. L.; Anderson, J. L. R.; Solomon, L. A.; Reddy, K. S.; Moser, C. C.; Dutton, P. L. *Nature* **2009**, *458*, 305.

(9) Bromley, E. H. C.; Channon, K.; Moutevelis, E.; Woolfson, D. N. *ACS Chem. Biol.* **2008**, *3*, 38.

(10) Fletcher, J. M.; Boyle, A. L.; Bruning, M.; Bartlett, G. J.; Vincent, T. L.; Zaccai, N. R.; Armstrong, C. T.; Bromley, E. H. C.; Booth, P. J.; Brady, R. L.; Thomson, A. R.; Woolfson, D. N. *ACS Synth. Biol.* **2012**, *1*, 240.

(11) (a) Boyle, A. L.; Bromley, E. H. C.; Bartlett, G. J.; Sessions, R. B.; Sharp, T. H.; Williams, C. L.; Curmi, P. M. G.; Forde, N. R.; Linke, H.; Woolfson, D. N. *J. Am. Chem. Soc.* **2012**, *134*, 15457. (b) Fletcher, J. M.; Harniman, R. L.; Barnes, F. R. H.; Boyle, A. L.; Collins, A.; Mantell, J.; Sharp, T. H.; Antognozzi, M.; Booth, P. J.; Linden, N.; Miles, M. J.; Sessions, R. B.; Verkade, P.; Woolfson, D. N. *Science* **2013**, *340*, 595.

(12) Armstrong, C. T.; Boyle, A. L.; Bromley, E. H. C.; Mahmoud, Z. N.; Smith, L.; Thomson, A. R.; Woolfson, D. N. *Faraday Discuss.* **2009**, *143*, 305.

(13) (a) Thomas, F.; Boyle, A. L.; Burton, A. J.; Woolfson, D. N. *J. Am. Chem. Soc.* **2013**, *135*, 5161. (b) Nautiyal, S.; Woolfson, D. N.; King, D. S.; Alber, T. *Biochemistry* **1995**, *34*, 11645.

(14) Zaccai, N. R.; Chi, B.; Thomson, A. R.; Boyle, A. L.; Bartlett, G. J.; Bruning, M.; Linden, N.; Sessions, R. B.; Booth, P. J.; Brady, R. L.; Woolfson, D. N. *Nat. Chem. Biol.* **2011**, *7*, 935.

(15) Marino, S. M.; Gladyshev, V. N. *J. Biol. Chem.* **2012**, *287*, 4419.

(16) (a) Akabas, M.; Stauffer, D.; Xu, M.; Karlin, A. *Science* **1992**, *258*, 307. (b) Weerapana, E.; Wang, C.; Simon, G. M.; Richter, F.; Khare, S.; Dillon, M. B. D.; Bachovchin, D. A.; Mowen, K.; Baker, D.; Cravatt, B. F. *Nature* **2010**, *468*, 790.

(17) (a) Sechi, S.; Chait, B. T. *Anal. Chem.* **1998**, *70*, 5150. (b) Creighton, T. E. *Nature* **1980**, *284*, 487.